Biomed Microdevices (2012) 14:1141–1148
DOI 10.1007/s10544-012-9680-5

Reliable permeability assay system in a microfluidic device mimicking cerebral vasculatures

Ju Hun Yeon · Dokyun Na · Kyungsun Choi · Seung-Wook Ryu · Chulhee Choi · Je-Kyun Park

Published online: 22 July 2012
© Springer Science+Business Media, LLC 2012

Abstract Since most of the bioavailable drugs are impermeable through the blood-brain barrier (BBB), development of a rapid and reliable permeability assay system has been a challenge in drug discovery targeting central nervous system (CNS). Here, we designed a microfluidic device to monitor the drug permeability into the CNS. Human umbilical vein endothelial cells (HUVECs) were shortly (2∼3 h) incubated with astrocyte-conditioned medium after being trapped on microholes in the microfluidic device and tested for chip-based permeability measurement of drugs. The measured permeability values were highly correlated with those measured by conventional *in vitro* methods and the brain uptake index representing the quantity of transported substances across the *in vivo* BBB of rats. Using the microfluidic device, we could easily monitor the effect of hydrogen peroxide on the trans-endothelial permeability, which are consistent with the finding that the same treatment disrupted the formation of tight junctions between endothelial cells. Considering relatively short period of time needed for endothelial cell culture and ability to monitor the BBB physiology continuously, we propose that this novel system can be used as an invaluable first-line tool for CNS-related drug development.

Keywords Blood–brain barrier · Microfluidics · Cell trapping · Permeability assay

J. H. Yeon · K. Choi · S.-W. Ryu · C. Choi (✉) · J.-K. Park (✉)
Department of Bio and Brain Engineering, KAIST,
291 Daehak-ro,
Yuseong-gu, Daejeon 305-701, Republic of Korea
e-mail: cchoi@kaist.ac.kr
e-mail: jekyun@kaist.ac.kr

D. Na
Department of Chemical and Biomolecular Engineering, KAIST,
291 Daehak-ro,
Yuseong-gu, Daejeon 305-701, Republic of Korea

S.-W. Ryu · C. Choi
KAIST Institute for the BioCentury,
291 Daehak-ro,
Yuseong-gu, Daejeon 305-701, Republic of Korea

J.-K. Park
KAIST Institute for the NanoCentury,
291 Daehak-ro,
Yuseong-gu, Daejeon 305-701, Republic of Korea

1 Introduction

Drug delivery from the blood into the central nervous system (CNS) is highly limited by the specialized structure termed the blood–brain barrier (BBB) (Pardridge et al. 1990). The BBB is composed of specialized brain microvascular endothelium and astroglial cell elements, which are in physical proximity to the vascular endothelium and basement membrane. The physicochemical properties of the BBB are essential for maintaining the CNS microenvironment for reliable neuronal activity (Cucullo et al. 2002; Abbott et al. 2006; Siddharthan et al. 2007). Therefore, any drug candidates for CNS application should be tested for the permeability through the BBB (Lundquist et al. 2002). Although assays using *in vivo* models provide the most reliable information, such approaches require frequent human intervention, skilled operation, and high cost. To overcome the technical difficulties of *in vivo* models, *in vitro* techniques determining BBB permeability have been developed (Lundquist et al. 2002). Such *in vitro* approaches have several advantages over *in vivo* models; they consume only small amounts of compounds and enable the development of high-throughput methodologies due to their relatively short assay time and convenient experimental handling (Nakagawa et al. 2009).

The reliability of *in vitro* BBB models can further be improved by utilizing a coculture system of endothelial cells and astrocytes, which increases the expression of dense tight

junctions, transporters, and enzyme systems by endothelial cells (Lundquist et al. 2002; Garcia et al. 2004; Abbott et al. 2006). Alternaltively, a flow-based *in vitro* BBB model using astrocyte-conditioned medium (ACM) was proposed to increase endothelial expression of zonular occludens (ZO-1) (Siddharthan et al. 2007). Ma et al. showed that cocultivation of endothelial cells and astrocytes on highly porous silicon nitride membranes increases direct interaction between endothelial cells and astrocytes, resulting in a better assay (Ma et al. 2005). Even though *in vitro* BBB models can be used as an alternative to *in vivo* models, they still require a long culture period for cells to form tight junctions between cells.

Here we present a permeability assay system using human umbilical vein endothelial cells (HUVECs) trapped in the microholes of a microfluidic device based on our previous report for measuring intestinal absorption using Caco-2 cells trapped in microholes (Yeon and Park 2009). By combination of trapping of endothelail cells and a short coculture with ACM, we could demonstrate that this device is useful for continuous monitoring of drug permeability through the BBB.

2 Materials and methods

2.1 Microfabrication process

The microfluidic device for the BBB permeability assay was fabricated using a multilayer lithography method as described previously (Yeon and Park 2009). Briefly, the microfluidic channel pattern was printed on a Cr mask. The mold master for the device was fabricated using a negative photoresist (SU-8 2005; MicroChem Corp., Newton, MA, USA) to manufacture microholes with conventional lithography. The second negative photoresist (SU-8 2025; MicroChem Corp.) was coated and exposed after aligning with the align mark of the first layer. After the second development, poly(dimethylsiloxane) (PDMS) prepolymer (Sylgard 184; Dow Corning) was mixed with a curing agent at a 10: 1 mass ratio and poured over the mold masters. Then, the PDMS structure was cured at 65 °C for 1 h and peeled from the mold. Consequently, the microholes were manufactured in the microfluidic device with a 45° angle.

2.2 Cell culture

Primary cultured HUVECs and human astrocytes (ScienCell, Gaithersburg, MD, USA) were selected for the BBB permeability assay (Ma et al. 2005). Cell layers cultured on Petri dishes were rinsed with phosphate-buffered saline (PBS) at pH 7.4 (Gibco, Grand Island, NY, USA). Then, trypsin-EDTA solution (0.25 % trypsin and 1 mM EDTA·4Na; Gibco) was used to detach the cells. EGM-2 (Lonza, Walkersville, MD, USA) and Dulbecco's modified Eagle's medium (DMEM; Gibco) supplemented with 20 % fetal bovine serum (FBS; Gibco) was added to the dispersed HUVEC cell layer and astrocytes, respectively. Cell cultures were maintained at 37 °C under 5 % CO_2 in a humidified water-jacketed incubator. We obtained ACM by cultivating astrocytes for 5 days. Prior to the permeability assay, appropriate aliquots of the HUVECs were refreshed and diluted to a suitable concentration of 2.5×10^6 cells/mL. Drug-treated cells and reagents were completely autoclaved after the experiments before discharge to ensure safety according to the KAIST experimental protocols for biosafety.

2.3 Experimental setup

The microfluidic devices were sterilized, and bubbles within channels were eliminated with 70 % ethanol for 10 min, followed by rinsing with cell culture media. HUVECs and astrocytes were incubated in the culture dishes, and 90 μL of medium and 10 μL of 1×10^7 cells/mL HUVECS were injected into inlet #1 of the microfluidic device (Fig. 1(b)). After trapping the HUVECs in the microholes, 100 μL of ACM from astrocytes cultured for 5 days was also injected into inlet #1. The drugs were injected into inlet #2 (Fig. 1(b)).

2.4 HPLC analysis

All drugs, including propranolol, antipyrine, carbamazepine, verapamil, and atenolol were purchased from Sigma–Aldrich. Other chemicals or reagents were purchased from Merck. The drug solution obtained after 2 h from outlet #1 was analyzed by reverse-phase high-performance liquid chromatography (HPLC) (Agilent 1100 series; Agilent Technologies, Santa Clara, CA, USA) with an Eclipse Plus C18 (5 μm, 4.6 mm×250 mm) column (Agilent Technologies). For HPLC analysis, 5-μL aliquots of the samples were applied, and buffers were passed through the column at a rate of 1 mL/min under isocratic conditions. The mobile phases were filtered through 0.46-μm sintered glass filters (Millipore, Bedford, MA, USA) and degassed in a sonicator (Branson, Danbury, CT, USA) before use. Drug concentrations were estimated from drug reference samples.

2.5 Data analysis

The effective permeability in the microfluidic device was calculated by the method developed previously (Yeon and Park 2009). Briefly, the effective permeability coefficient (P_{eff}) at the steady-state condition was derived from the conventional equation for adapting a microfluidic perfusion system (Grassi and Cadelli 2001; Hubatsch et al. 2007):

$$P_{\text{eff}} = \frac{1}{AC_0}\frac{\partial Q}{\partial t} \tag{1}$$

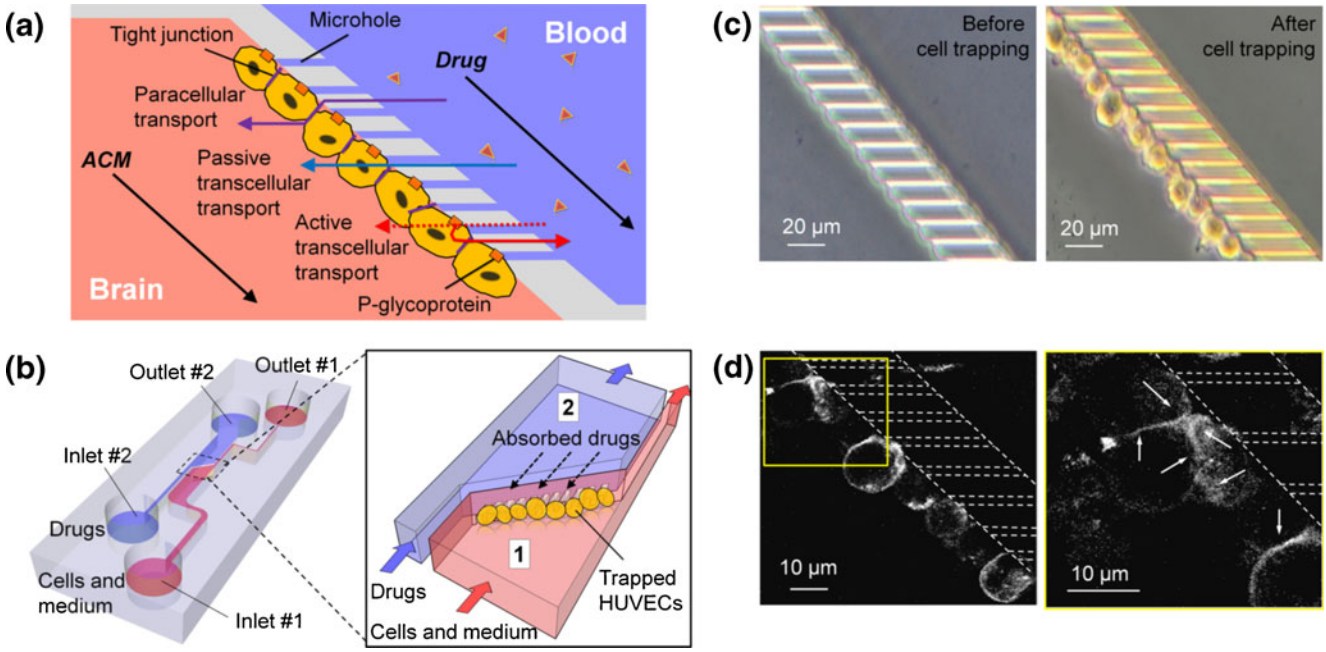

Fig. 1 Device concept of a microfluidic device for the blood–brain barrier (BBB) model study and HUVECs trapped on the microholes of a microfluidic device. (**a**) Design of microfluidic device mimicking the BBB model and diverse drug transport routes across HUVECs trapped in microholes. (**b**) Schematics of the microfluidic device. Suspended HUVECs in culture media are injected and trapped in the microhole array. Then, drugs are absorbed by the trapped cells through the holes. (**c**) HUVECs trapped on the microholes are in tight contact with each other. (**d**) Tight junctions between HUVECs trapped on the microhole array were stained with ZO-1 monoclonal antibody, which was tagged with Alexa Fluor 594. Arrows in the magnified image indicate tight junctions between cells stained with the ZO-1 antibody

where P_{eff} is the permeability (cm/s), A is the surface area (cm^2), C_0 is the initial drug concentration (mM), and Q is the number of absorbed molecules (mole). The surface area (A) was determined by multiplying the number of holes in the microhole array (76 trapping holes) by the area of each hole (1.5×10^{-7} cm^2). From Eq. 1, we derived the effective permeability equation as follows:

$$P_{\text{eff}} = \nu \frac{C}{C_0} \frac{1}{A} \tag{2}$$

where ν=10 cm^3/s (flow rate within the microfluidic channel), A=1.2×10^{-5} cm^2 (surface area of microholes). C_0, is the initial concentration of applied drug. C is the concentation of absorbed drugs after 2 h.

2.6 Immunofluorescent staining of cell junction protein

HUVECs trapped on microholes in a microfluidic device or grown on coverslipswere fixed in 4 % paraformaldehyde for 15 min at room temperature. After washing three times with PBS for 5 min each, the cells were permeabilized with 0.15 % Triton X-100 for 15 min. Then, the cells were blocked for 1 h in a PBS solution containing 3 % BSA (Sigma–Aldrich). The cells were stained with Alexa fluor® 594-tagged ZO-1, which was conjugated with mouse monoclonal antibody (Molecular Probes), diluted 1:50, and incubated for 2 h at room temperature (Tang 2006; Siddharthan et al. 2007). The cells were again washed three times in PBS before being mounted onto the stage of a confocal microscope (Axiovert 25; Carl Zeiss, Germany).

3 Results

3.1 Device configuration and cell trapping in microholes

Unlike conventional permeability assay systems requiring embedded membrane structures for mimicking a cell monolayer, we designed a microhole structure for trapping HUVECs in the microdevice based on our previous study (Yeon and Park 2009). Drugs can be transported through various routes including transcellular pathways and a paracellular pathway between cells in a microfluidic device (Fig. 1(a)). The microfluidic device includes two inlet ports, two outlet ports, and a microhole array for cell trapping (Fig. 1(b)). HUVECs were supplied from inlet #1 to outlet #1 at a flow rate of 20 μL/h, whereas fresh medium was supplied from inlet #2 to outlet #2 at the same flow rate. Once infused into inlet #1, HUVECs were automatically trapped on the microholes due to the pressure gradient between the two sides of the microhole array. The pressure gradient was formed due to differential flow velocity in the microfluidic channels. After spontaneous cell trapping, ACM was constantly supplied with 10 μL/h of flow rate

along the microfluidic channel for reducing the shear stress on trapped cells by decreasing the flow rate and the pressure difference between region 1 and region 2. Also, this continuous flow of ACM can affect HUVECs to realize *in vivo*-like fluidic environment.

Shear stress in blood veins ranges between 1 – 6 dynes/ cm^2. In our system, the range of shear stress is 0.28 to 8.19 dynes/ cm^2, which is comparable with *in vivo* shear stress in blood vessel. Shear stress is calculated using below equation (Papaioannou and Stefanadis 2005).

$$\tau = \frac{6\mu Q}{h^2 w}$$

τ denotes shear stress, μ viscosity of HUVEC media (7.9×10^{-3} dynes·s/cm^2) (Abaci et al. 2012), Q volumetric flow rate (2.7×10^{-6} cm^3/s), h height of microfluidic channel (2.5×10^{-3} cm), w width of microfluidic channel (2.5×10^{-3} – 7.37×10^{-2} cm).

Incubation with ACM is known to induce expression of tight junction proteins (Tang 2006; Barar and Omidi 2008), P-glycoprotein (Fenart et al. 1998; Gaillard et al. 2000), and membrane receptors by endothelial cells (Abbott et al. 2006). To test the integrity of trapped HUVECs, cells were monitored under the microscope during the incubation with ACM (Fig. 1(c)). Two hours after trapping and subsequent incubation with ACM, cells trapped on the microholes were tested for expression of ZO-1, a major component of tight junctions, by immunofluorescence staining. Drugs are then infused into inlet #2, and the fraction transported from region 2 to region 1 via endothelial absorption can be gathered at outlet #1 (see the magnified picture in Fig. 1(b)) and 10 μL of transported drugs was taken out every hour. The concentration of transported drugs was determined by reverse-phase HPLC.

3.2 Effect of ACM on drug permeability in a microfluidic device

To investigate the flow stream difference before and after trapping cells, we injected medium into inlet #1 and FITC-dextran into the inlet #2, separately. In the absence of trapped cells on the microholes, the medium flowed through the microholes and FITC-dextran was swept away from the microholes because the pressure of region 1 is higher than that of region 2 (Fig. 2(a)). In the presence of trapped cells, the holes were blocked and thereby FITC-dextran moved along the microholes. Then, FITC-dextran in contact with cells in the microholes was transported into the region 1. In case of microhole leakage due to failure in perfect cell trapping over all microholes, the flow moving through the microhole prevented the move of FITC-dextran to the region 1. This characteristic pattern makes our microfluidic device robust by avoiding detection error caused by leakage.

For monitoring the transport through the trapped endothelial cells in the microdevice, we utilized Evans blue dye, a widely used dye for assaying BBB permeability (Aoki et al. 2002; Ay et al. 2008; Patel et al. 2008). Incubation with ACM for 2 h induced a significant decrease in dye permeability through trapped HUVECs compared to the untreated control (Fig. 3(a)), which is in good agreement with the observation that ACM enhanced the expression of tight junction protein in the trapped HUVECs. It has been shown that the addition of soluble factors derived from the cultures of human astrocytes and microglia significantly decrease the permeability of endothelial cell monolayers to large macromolecules within 2–3 h (Prat et al. 2001). It has also been demonstrated that the dynamics of potassium movement across *in vitro* BBB by measuring the rate of potassium efflux from the extra-capillary space (Stanness et al. 1997). When co-cultured with astrocytes, the potasium efflux through endothelial cells was significantly decreased within 1 h and such effect was maintained for two weeks. Also, trans-epithelial electric resistance (TEER) value rapidly increased within 20 min after co-culture with astrocytes.

To further characterize the effect of hydrodynamic diameters of transported molecules, we tested FITC-dextran with various molecular mass for the trans-endothelial transport in the device. As expected, the permeability of FITC-dextran was inversely correlated with its molecular weight (Fig. 3(b)). Since large dextrans (70 kDa) were impermeable even in the absence of ACM, the effect of ACM incubation was only observed in 4 and 40 kDa FITC-dextrans.

3.3 Comparison of the permeability values measured in the device with conventional methods

To validate the reliability of our proposed device, we tested five well-known drugs. The permeability values of carbamazepine, verapamil, and atenolol significantly decreased when ACM was supplemented into the microfluidic channel (Fig. 4(a)). However, the permeability difference was negligible in case of propranolol. Propranolol is highly permeable, so the drug would permeate well even in the presence of tight junctions.

Effective drug permeability P_e (cm/s) was calculated by Eq. 2 described in Experimental. The incubation with ACM significantly lowered the P_e value of drugs compared to that of HUVECs alone in a microfluidic device (Table 1). The P_e of propranolol was only slightly decreased by the incubation with ACM consistent with previous result.

The permeability values were also compared with those available from the literature, which were measured *in vitro* by co-culturing HUVECs and astrocytes on porous membrane. For antipyrine, carbamazepine and atenolol, the P_e values of measured in the *in vitro* BBB system were comparable to those measured with microfluidic device of

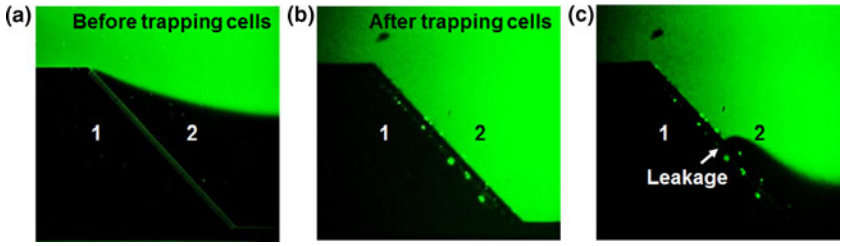

Fig. 2 The difference of flow stream before and after cell trapping. (**a**) No cell was trapped in the microholes and thereby buffer flows from region 1 to region 2 through the microholes. (**b**) The microholes were blocked by trapped cells which prevent the flow from the region 1 to 2. (**c**) The lower part of the holes was not blocked by cells, which results in buffer flow through the free holes

HUVECS supplemented with ACM. For propranolol and verapamil, which are inducers of P-glycoprotein and actively transported drugs, the P_e in the device was higher than that in a conventional *in vitro* BBB model. As shown in Fig. 4(b), the P_e values measured in the device and the P_e values of the *in vitro* BBB model were strongly correlated (R^2=0.998). In addition, we compared the brain uptake index (BUI) with the P_e measured in the microfluidic device because BUI represents the actual drug absorption in the BBB model as follows:

$$BUI = \frac{Brain^{14}C/Brain^{3}H \times 100}{Injected^{14}C/Injected^{3}H} \quad (3)$$

As shown in Fig. 3(c), the permeability measured in the microfluidic device and the BUI were correlated with R^2=0.6859 (Lundquist et al. 2002).

3.4 Real-time monitoring the effect of hydrogen peroxide on endothealial permeability

Breakdown of BBB has been regarded as a hallmark in a variety of neurological conditions such as traumatic brain injury, multiple sclerosis, stroke and malignancies. A common feature in all these condition is the imbalance in the oxidant–antioxidant system, resulting in excessive accumulation of reactive oxygen species (ROS) inside or outside of neuronal cells. Besides other detrimental effects, ROS have been shown to disrupt BBB integrity by influencing ZO protein distribution (Pun et al. 2009). To test the effect of hydrogen peroxide on ZO protein expression, we incubated HUVECs on a Petri dish in the absence or presence of ACM and then added 100 μM hydrogen peroxide for an additional 2 h. As shown in Fig. 5(a) and (b), incubation with ACM enhanced the formation of tight junctions between endothelial cells; while treatment with hydrogen peroxide prominently decreased the membrane localization of ZO-1 and subsequent detachment from neighboring endothelial cells. Next, we measured the effect of hydrogen peroxide on HUVEC permeability over time using the microdevice for 6 h. Addition of low concentration of hydrogen peroxide (50 μM) did not affect the transport kinetics of FITC-dextran through the trapped HUVECs (Fig. 4(c)); while administration of high dose of hydrogen peroxide (100 μM) instantly increased the permeability for dextran (Fig. 4(d)).

4 Discussion

We developed a microfluidic device for permeability assays mimicking the BBB model. In addition to ACM incubation,

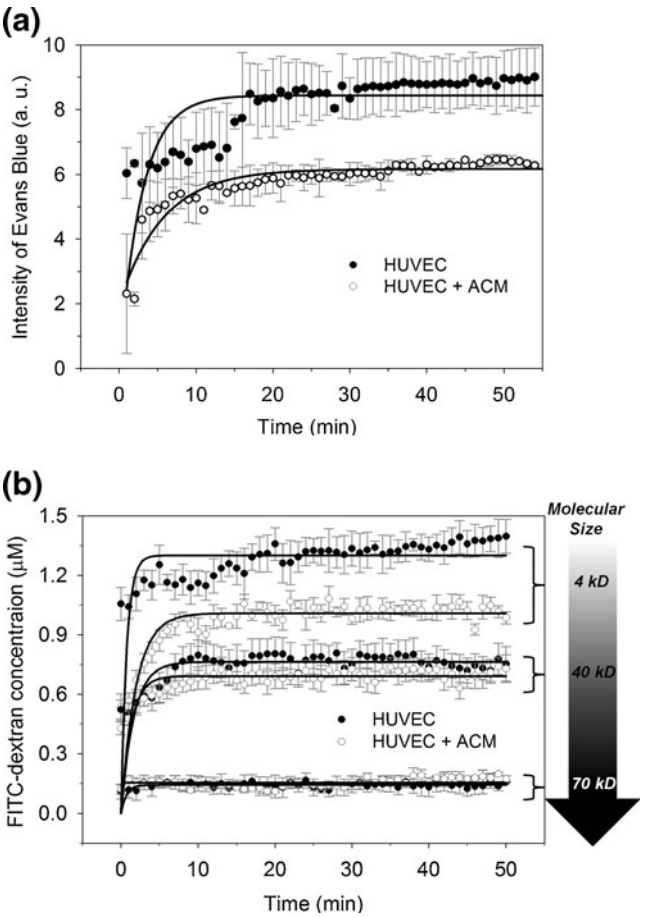

Fig. 3 The transport of Evans blue dye and FITC-dextran through trapped HUVECs. The permeability of Evans blue dye (**a**) and dextrans with various molecular weights (**b**) between HUVECs treated with astrocyte-conditioned medium (ACM) and those without ACM. Evans blue intensity was expressed as an arbitrary unit (n=3)

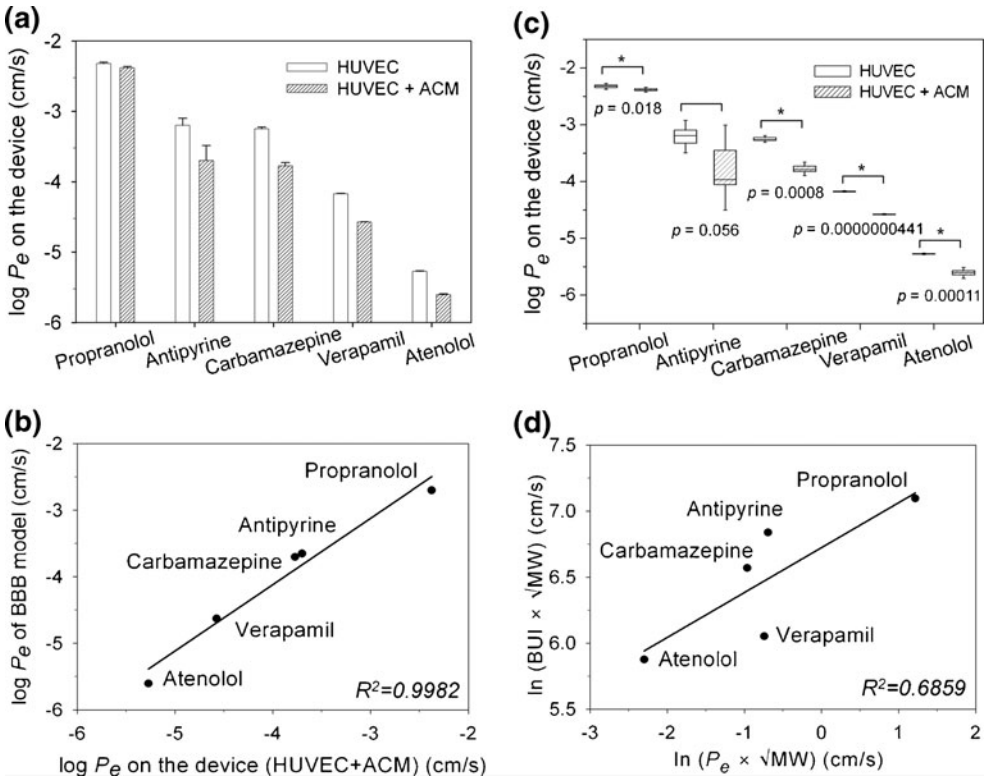

Fig. 4 Statistical analysis of the permeability assay results. (**a**) Comparison of the effective permeability (Pe) on the device using HUVECs in the absence or presence of ACM. *p values from t-test <0.05 ($n \geq 3$). (**b**) Comparison of drug permeability values measured in the microfluidic device *vs*. the *in vitro* BBB model. (**c**) Comparison of drug permeability values measured in the device vs. brain uptake index (BUI)

we tried to apply the shear stress to the trapped HUVECs in microholes to realize an *in vivo*-like microenvironment in a microfluidic device as the endothelial linings are continuously exposed to blood flow *in vivo*. The permeability values measured in our microfluidic device showed good agreement with the *in vivo* permeability data, indicating that our device can be used to predict the CNS permeability of the investigational drugs. Although the proposed permeability assay system lacks several key features of *in vivo* BBB model such as the interactions and three dimentional configuration of brain capillary enthothelial cells, astroytes, and pericytes, this system has an advantage over conventional *in vivo* and *in vitro* models: dramatically reduce assay time due to the nonnecessity for long-term cell culture in the device and observe the BBB permeability continuosly change over time.

Several *in vitro* BBB models have been developed using immortalized endothelial cell lines or cultured primary endothelial cells. Assays with cell lines such as human colon carcinoma cells (Caco-2) and Madin–Darby canine kidney (MDCK) cells rather than primary endothelial cells have resulted in different permeability values from *in vivo* values, as those cells do not form a robust tight junction which is crucial for a BBB permeability assay (Abbott 2004). Early passages of primary endothelial cell cultures help maintain the key features of the *in vivo* BBB such as tight junctions, transporters, enzymes, and receptors (Nakagawa et al. 2009). Therefore, membrane-based *in vitro* models using primary endothelial cells have been widely used to study the biology of the BBB and to measure the permeability of potential chemicals. However, primary endothelial cells quickly lose

Table 1 Comparison among P_e in the microfluidic device, P_e in the device with HUVEC and ACM, only HUVEC, P_e of *in vitro* BBB, and brain uptake index (BUI) (n=3)[a]

Compound	P_e in the device (cm/s)		P_e of *in vitro*	BUI (%)
	HUVEC+ACM	HUVEC	BBB (cm/s)	
Propranolol	4.21e−3±0.16e−3	4.77e−4±0.16e−3	1.9872e−3 (Nakagawa et al. 2009)	75 (Lundquist et al. 2002)
Antipyrine	1.99e−4±1.27e−4	5.57e−4±1.27e−4	2.2251e−4 (Nakagawa et al. 2009)	68 (Lundquist et al. 2002)
Carbamazepine	1.69e−4±0.19e−4	5.67e−4±0.19e−4	1.9853e−4 (Nakagawa et al. 2009)	31 (Lundquist et al. 2002)
Verpamil	2.66e−5±0.02e−5	6.73e−5±0.02e−5	2.3510e−5 (Nakagawa et al. 2009)	52 (Betzen et al. 2009)
Atenolol	2.48e−6±0.22e−6	5.35e−6±0.22e−6	2.4900e−6 (Nakagawa et al. 2009)	26 (van de Waterbeemd et al. 1998)

[a] *HUVEC* human umbilical vein endothelial cells; *ACM* astrocyte-conditioned medium; *BBB* blood–brain barrier

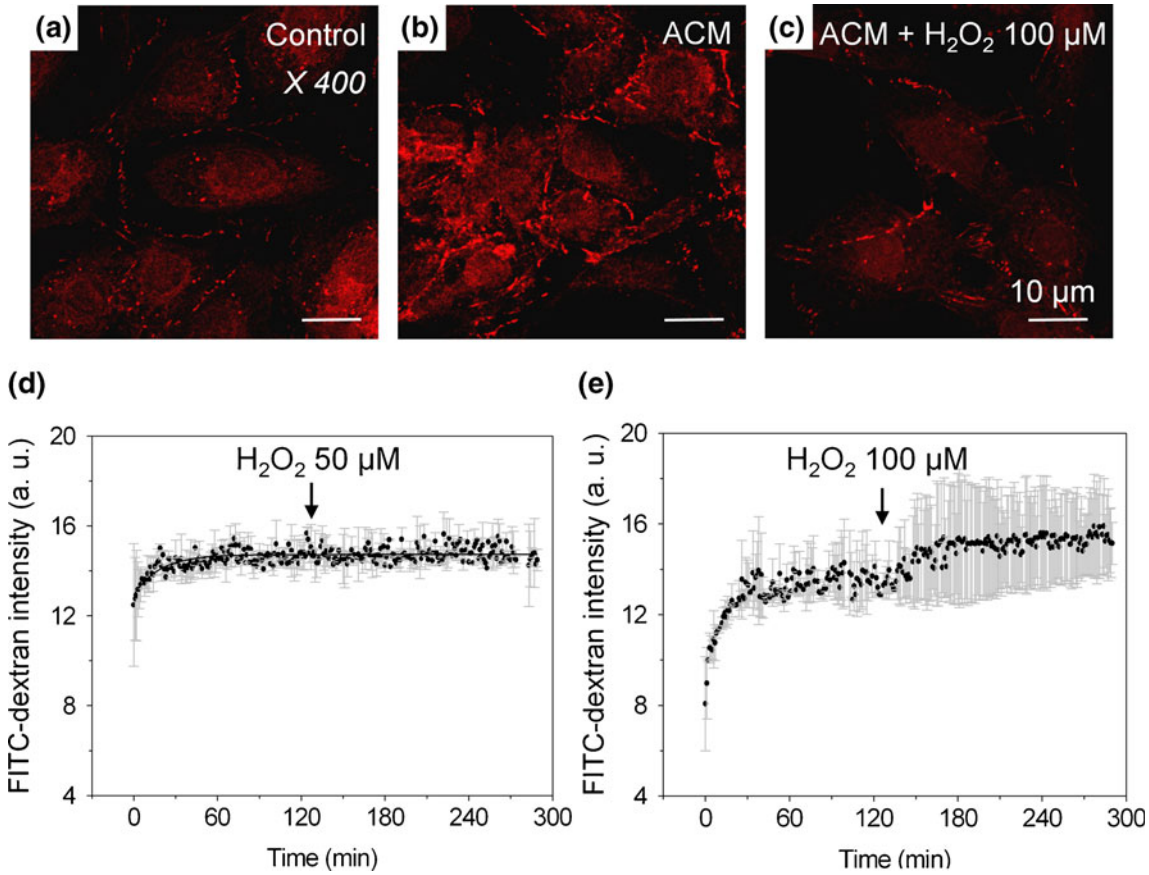

Fig. 5 The effect of hydrogen peroxide on permeability of HUVECs supplemented with ACM. The expression of zonular occludens tight junction protein (ZO-1) by HUVECs cultured with control media (**a**), HUVECs cultured with ACM (**b**), and HUVECs cultured with ACM followed by treatment with 100 μmol/L of hydrogen peroxide (**c**). Permeability of dextran was measured after adding 50 (**d**) or 100 μmol/L (**e**) of hydrogen peroxide. FITC-dextran intensity was expressed in arbitrary unit (a.u.)

their BBB biological characteristics when isolated and cultured alone, since the interaction between the brain endothelium and surrounding astrocytes within neurovascular units is essential for the formation and maintenance of the BBB.

We have incubated the trapped HUVECs with ACM as short as two hours to assay BBB permeability and drug absorption in our device because the effect of astrocyte-derived soluble factors on endothelial cell layers starts to appear within 2 h (Stanness et al. 1997; Prat et al. 2001). It has also been reported that permeability decreases when endothelial cells and astrocytes are co-cultured for 2 h (Stanness et al. 1997; Sobue et al. 1999). Astrocytes help endothelial cells maintain their BBB properties by upregulating P-glycoprotein on endothelial cells. In contrast, non-contact cocultivation of astrocytes enhances transendothelial resistance and decreases transendothelial permeability in an *in vitro* BBB model (Garcia et al. 2004; Siddharthan et al. 2007; Nakagawa et al. 2009). Astrocytes do not make direct contact with endothelial cells *in vivo*, but are separated from endothelial cells by an extracellular matrix. However, the chemical nature of the astrocyte-produced signals for inducing and maintaining HUVEC barrier properties is unclear. Several candidate molecules have been identified, such as tumor growth factor-β and basic fibroblast growth factor, which upregulate barrier properties by increasing resistance and decreasing paracellular permeability in brain endothelial cells (Siddharthan et al. 2007).

Previous studies have suggested that the permeability of endothelial and epithelial cells is regulated by components of tight and adherent junction proteins such as ZO-1, occludin, and claudin (Siddharthan et al. 2007). In particular, ZO-1 is a protein participating in the specialized cell–cell interactions between endothelial cells. We confirmed the formation of tight junctions between HUVECs trapped in the microhole array of a microfluidic device after supplementing them with ACM for 2 h. The ZO-1 protein was produced more in the junction between HUVECs than on the surface of single HUVEC membranes and was also expressed on the contact area between cells and the microhole array surface. We also confirmed that brief exposure to hydrogen peroxide, a major mediator of ROS *in vivo*, led to a redistribution of ZO-1 from the tight junction to the cytosol, resulting in a decrease in BBB

permeability in our device (Yeh et al. 2007; Betzen et al. 2009). Although ROS are key mediators of BBB breakdown and implicate antioxidants as potential neuroprotectants in stroke and traumatic brain injury, the mechanisms by ROS which may induce an increase in vascular permeability are not clearly understood (Lee et al. 2004; Pun et al. 2009). Although we observed an effect of hydrogen peroxide on BBB permeability using a microfluidic device, it will be valuable to investigate the effect of antioxidants such as vitamin E, which is a homeostatic factor that helps to prevent microvascular leakage and permeability defects, and selenium, which detoxifies lipoperoxides and hydrogen peroxide (Öztas et al. 2000; Yu and Adedoyin 2003).

Using the trapped HUVECs supplemented with ACM mimicking the BBB model, an integrated system including a toxicity assay and metabolism assay, would be a valuable tool for development of CNS-targeted drugs and studying the pathophysiological changes induced by reactive oxygens. The applicability of this integrated assay system can be extended to measure absorption, distribution, metabolism, excretion, and toxicity (ADME/Tox) of drugs.

Acknowledgements This research was supported by a National Research Laboratory (NRL) Program grant (2011-0018607), a Converging Research Center Program grant (2011K000864) through the National Research Foundation and a grant (2009 K001282) from the Brain Research Center of the 21st Century Frontier Research Program funded by the Ministry of Education, Science and Technology (MEST) of Republic of Korea.

References

H.E. Abaci, R. Devendra, Q. Smith, S. Gerecht, G. Drazer, Biomed. Microdev. **14**, 145 (2012)
N.J. Abbott, Drug Discov Today **1**, 407 (2004)
N.J. Abbott, L. Rönnbäck, E. Hansson, Nat. Rev. Neurosci. **7**, 41 (2006)
T. Aoki, T. Sumii, T. Mori, X. Wang, E.H. Lo, Stroke **33**, 2711 (2002)
I. Ay, J.W. Francis, H. Brown Jr., Brain Res. **1234**, 198 (2008)
J. Barar, Y. Omidi, J. Biol. Sci. **8**, 556 (2008)
C. Betzen, R. White, C.M. Zehendner, E. Pietrowski, B. Bender, H.J. Luhmann, C.R.W. Kuhlmann, Free Radic. Biol. Med. **47**, 1212 (2009)
L. Cucullo, M.S. McAllister, K. Kight, L. Krizanac-Bengez, M. Marroni, M.R. Mayberg, K.A. Stanness, D. Janigro, Brain Res. **951**, 243 (2002)
L. Fenart, V. Buee-Scherrer, L. Descamps, C. Duhem, M.-G. Poullain, R. Cecchelli, M.-P. Dehouck, Pharm. Res. **15**, 993 (1998)
P.J. Gaillard, I.C.J. van der Sandt, L.H. Voorwinden, D. Vu, J.L. Nielsen, A.G. de Boer, D.D. Breimer, Pharm. Res. **17**, 1198 (2000)
C.M. Garcia, D.C. Darland, L.J. Massingham, P.A. D'Amore, Dev Brain Res **152**, 25 (2004)
M. Grassi, G. Cadelli, Int. J. Pharm. **229**, 95 (2001)
I. Hubatsch, E.G.E. Ragnarsson, P. Artursson, Nat. Protoc. **2**, 2111 (2007)
H.-S. Lee, K. Namkoong, D.-H. Kim, K.-J. Kim, Y.-H. Cheong, S.-S. Kim, W.-B. Lee, K.-Y. Kim, Microvasc. Res **68**, 231 (2004)
S. Lundquist, M. Renftel, J. Brillault, L. Fenart, R. Cecchelli, M.-P. Dehouck, Pharm. Res. **19**, 976 (2002)
S.H. Ma, L.A. Lepak, R.J. Hussain, W. Shain, M.L. Shuler, Lab Chip **5**, 74 (2005)
S. Nakagawa, M.A. Deli, H. Kawaguchi, T. Shimizudani, T. Shimono, K. Kittel, K. Tanaka, M. Niwa, Neurochem. Int. **54**, 253 (2009)
B. Öztas, E. Erkin, E. Dural, T. Isbir, Int. J. Neurosci. **105**, 27 (2000)
T.G. Papaioannou, C. Stefanadis, Hell. J. Cardiol. **46**, 9 (2005)
W.M. Pardridge, D. Triguero, J. Yang, P.A. Cancilla, J. Pharmacol. Exp. Ther. **253**, 884 (1990)
T.H. Patel, S. Sprague, Q. Lai, D.F. Jimenez, C.M. Barone, Y. Dingb, Neurosci. Lett. **444**, 222 (2008)
A. Prat, K. Biernacki, K. Wosik, J.P. Antel, Glia **36**, 145 (2001)
P.B.L. Pun, J. Lu, S. Moochhala, Free Radic. Biol. Med. **43**, 348 (2009)
V. Siddharthan, Y.V. Kim, S. Liu, K.S. Kim, Brain Res **1147**, 39 (2007)
K. Sobue, N. Yamamoto, K. Yoneda, M.E. Hodgson, K. Yamashiro, N. Tsuruoka, T. Tsuda, H. Katsuya, Y. Miura, K. Asai, T. Kato, Neurosci. Res. **35**, 155 (1999)
K.A. Stanness, L.E. Westrum, E. Fornaciari, P. Mascagni, J.A. Nelson, S.G. Stenglein, T. Myers, D. Janigro, Brain Res **771**, 329 (1997)
V.W. Tang, Biol Direct **1**, 1 (2006)
H. van de Waterbeemd, G. Camenisch, G. Folkers, J.R. Chretien, O.A. Raevsky, J Drug Targeting **6**, 151 (1998)
W.-L. Yeh, D.-Y. Lu, C.-J. Lin, H.-C. Liou, W.-M. Fu, Mol. Pharmacol. **72**, 440 (2007)
J.H. Yeon, J.-K. Park, Anal. Chem. **81**, 1944 (2009)
H. Yu, A. Adedoyin, Drug Discov today **8**, 852 (2003)